Acta Crystallographica Section B
Structural Science
ISSN 0108-7681

Disorder of $(NH_4)_3H(SO_4)_2$ in the high-temperature phase I

Yoo Jung Sohn,[a]* Karine M. Sparta,[a] Martin Meven[b] and Gernot Heger[a]

[a]RWTH Aachen University, Institut für Kristallographie, Jägerstrasse 17-19, 52056 Aachen Germany, and [b]ZWE FRM-II, TU München, Lichtenbergerstrasse 1, 85747 Garching, Germany

Correspondence e-mail: sohn@xtal.rwth-aachen.de

Received 22 November 2010
Accepted 25 February 2011

The highly disordered crystal structure of triammonium hydrogen disulfate, $(NH_4)_3H(SO_4)_2$, in the high-temperature phase I was studied using single-crystal neutron diffraction. It is known that the O atom involved in hydrogen bonding between neighbouring SO_4 tetrahedra is disordered and takes a split-atom position, building a two-dimensional hydrogen-bond network in the (001) plane. The H atoms in these SO_4–H—SO_4 hydrogen bonds are disordered and hence refined with a split-atom model. Moreover, from the much larger anisotropic mean-square displacements of ammonium protons the NH_4^+ groups were refined with a reasonable split-atom model, and their motional behaviour was also analysed by rigid-body treatment. Finally, careful consideration was given to show possible supplementary proton migration between the ammonium protons and those of the hydrogen bonds in this high-temperature phase.

1. Introduction

With five successive structural phase transitions, triammonium hydrogen disulfate, $(NH_4)_3H(SO_4)_2$ (TAHS), shows the richest polymorphism among the compounds with the general formula $M_3H(XO_4)_2$ (M = NH_4^+, K^+, Rb^+, Cs^+; X = S, Se; Gossner, 1904; Fischer, 1914; Gesi, 1976, 1980). The characteristic feature of these compounds is the strong hydrogen bond between two XO_4^{2-} ions forming a $(XO_4)H(XO_4)$ dimer. The high-temperature phase I of TAHS above 413 K crystallizes in the space group $R\bar{3}m$ (No. 166; Hahn, 2002) and is well known for its superprotonic conductivity (Schwalowsky *et al.*, 1998; Chen *et al.*, 2000). This high protonic conductivity in the (001) plane of the hexagonal lattice ($10^{-2} \leq \sigma_{(001)} \leq 10^{-1}$ S cm^{-1}) is due to the disordered hydrogen-bond networks which allow a fast proton diffusion (Baranov, 2003). While isolated hydrogen-bonded $(SO_4)H(SO_4)$ dimers are characteristic for the crystal structure of the low-temperature phases TAHS II–V, a two-dimensional pseudo-hexagonal network of hydrogen bonds between the SO_4 groups is formed in the high-temperature phase I of TAHS.

A detailed crystal structure analysis of TAHS-I by X-ray diffraction was carried out by Friese *et al.* (2002). The rhombohedral structure (space group $R\bar{3}m$) consists of SO_4 tetrahedra linked to each other *via* H1 atoms, forming a hydrogen-bond network in the (001) plane. The $N1H_4^+$ groups lie at the centre of a six-membered ring within the O1—H1—O1 hydrogen-bond network. The O1 atoms of the SO_4 tetrahedra are alternately oriented up and down with respect to the c axis. These SO_4–H–SO_4 sandwich structures perpendicular to c are separated by double layers of $N2H_4^+$ tetrahedra with alter-

© 2011 International Union of Crystallography
Printed in Singapore – all rights reserved

Table 1
Experimental details of single-crystal neutron diffraction.

Crystal data	
Chemical formula	$HO_8S_2{\cdot}3H_4N$
M_r	247.2
Crystal system, space group	Trigonal, $R\bar{3}m$
Temperature (K)	413
a, c (Å)	5.907 (3), 22.57 (1)
V (Å^3)	682.0 (6)
Z	3
Radiation type	Neutron, λ = 0.555 Å
μ (mm^{-1})	0.017
Crystal size (mm)	3 × 3 × 3
Data collection	
Diffractometer	Single-crystal HEiDi
Absorption correction	None
No. of measured, independent and observed [$I>3\sigma(I)$] reflections	1164, 452, 133
R_{int}	0.065
Refinement	
$R[F^2>3\sigma(F^2)]$, $wR(F^2)$, S	0.056, 0.109, 1.51
No. of reflections	452
No. of parameters	48
No. of restraints	0
H-atom treatment	All H-atom parameters refined
$\Delta\rho_{max}$, $\Delta\rho_{min}$ (barn Å^{-3})	4.89, −3.51

Computer programs used: *DIF4N* (modified Linux version of *DIF*4), *PRON* (Scherf, 1998), *JANA*2006 (Petricek *et al.*, 2006), *ATOMS*5.1 (Dowty, 2000).

nating hydrogen configurations. N1 is coordinated by the H2 and H3 atoms, N2 by the H4 and H5 atoms. One remarkable feature of the TAHS-I structure is the disordering of the O1 atom which is involved in hydrogen bonding. Rather than lying on a threefold axis, O1 is slightly shifted and occupies three split-atom positions. The H1 atom of the hydrogen bond lies on a 9*e* Wyckoff position, whereas only one-third of the nine possible sites are occupied. This allows the H atoms to move almost freely between energetically equivalent positions. Moreover, according to NMR studies on TAHS-I a chemical exchange between the ammonium protons[1] and the protons involved in the hydrogen bond of SO_4–H–SO_4 has been suggested (Fechtelkord *et al.*, 2000). This observation also supports proton conduction in the (001) plane as assumed by Merinov *et al.* (2000).

Our previous investigation of TAHS-II by single-crystal neutron diffraction at room temperature showed a disordering of the H atom of $(SO_4)H(SO_4)$ around the inversion centre in the middle of the dimer (Sohn *et al.*, 2009). In the structure analysis this disordered H atom was refined using a split-atom model. We also observed increased anisotropic mean-square displacements for the protons of the NH_4^+ groups, indicating a reorientational disorder due to competing N—H···O hydrogen bonds with adjacent SO_4 tetrahedra.

Detailed structure analyses of the low-temperature phases II–V of TAHS by single-crystal X-ray diffraction were carried out by Dominiak *et al.* (2003). They observed additional weak interlayered reflections which may result from a modulation of the crystal structure. We tried to verify this observation for phase II at room temperature by similar X-ray diffraction studies using an image-plate diffractometer (Stoe IPDS). The observed weak reflections disappeared in our experiments when lowering the voltage from 35 to 30 kV, which is clearly an indication of a $\lambda/2$ contamination effect (the energy of Mo $K\alpha_1$ is 17.480 keV).

In order to understand the highly disordered crystal structure of TAHS-I, especially regarding the proton distribution, we carried out single-crystal neutron diffraction studies. The characteristic proton disorder of TAHS-I was compared with that of TAHS-II. An additional analysis of the NH_4^+ groups with a rigid-body treatment using TLS parameters provides a rough description of their translational and librational behaviour with respect to the crystallographic axes. Finally, a possible pathway of superprotonic conductivity is discussed according to the results of the crystal structure analysis.

2. Experimental

Single TAHS crystals of optical quality were grown from aqueous solution by slow evaporation. Samples of typically 3 × 3 × 3 mm were used for single-crystal neutron diffraction experiments. Test experiments have shown that our large, almost perfect TAHS crystals were damaged or even broken when heating through the $C2/c$–$R\bar{3}m$ phase transition. This strain-induced effect can be avoided by using a crystal which consists of twin domains in the monoclinic TAHS-II phase at room temperature. Slow heating through the phase transition leads to a monodomain single crystal in the TAHS-I phase. A complete dataset of Bragg reflection intensities was collected up to $(\sin\theta/\lambda)_{max}$ = 0.9 Å^{-1} on the four-circle diffractometer HEiDi at the FRM II in Garching with a wavelength of λ = 0.555 Å [Cu(420) monochromator] at 413 K. A small cylindrical, thin-walled Al furnace with a NiCr/Ni thermocouple as the temperature sensor was used (Heger *et al.*, 1975). With this unit we achieved a long-term temperature stability of ± 2 K. Data reduction was performed with the program *PRON* (Scherf, 1998). No absorption correction was made due to the small linear absorption coefficient (∼ 0.017 mm^{-1}). Structure refinement was carried out using *JANA*2006 (Petricek *et al.*, 2006). The spherical shell model for a freely rotating $N1H_4^+$ group was refined with *FULLPROF* (Rodriguez-Carvajal, 2001). Experimental details are given in Table 1.[2]

3. Results and discussion

3.1. Crystal structure of TAHS-I: conventional model

The crystal structure of TAHS-I is rhombohedral, space group $R\bar{3}m$. The lattice parameters used in the refinements were taken from our previous X-ray powder measurements (Sohn *et al.*, 2009) and are (in hexagonal setting) a = 5.907 (3), c = 22.57 (1) Å. These values were chosen because they are

[1] Neutron diffraction probes the core density distribution of atoms and not their density. Therefore, for H atoms only the proton distribution is obtained in a structure analysis by neutron diffraction.

[2] Supplementary data for this paper are available from the IUCr electronic archives (Reference: EB5009). Services for accessing these data are described at the back of the journal.

Table 2
Hydrogen bond lengths (Å) in TAHS-I and TAHS-II.

	TAHS-I (conventional model)	TAHS-I†	TAHS-II†
O1—H1	1.323 (7)	0.99 (2)	0.99 (1)
H1—H1	0	0.75 (2)	0.57 (1)
O1—O1	2.646 (1)	2.675 (8)	2.549 (7)

† Split-atom model.

more precise than the lattice parameters a_n and c_n from the single-crystal neutron diffraction measurement, which are still in agreement with the powder results within one standard deviation: a_n = 5.89 (4) and c_n = 22.51 (7) Å.

The neutron structure refinement was started with a 'conventional' model according to the work by Friese *et al.* (2002), in which only O1 and H3 atoms were split. All the atoms except H3 were treated anisotropically. The result yields well localized S, N and O atoms with rather small, almost spherical mean-square displacements. All H atoms except H3 show strongly enlarged anisotropic mean-square displacements. The final *R* factor was 0.1288 with 43 refinement parameters.

3.2. Crystal structure of TAHS-I: split-atom model

A difference-Fourier map suggests further splitting of the H1 protons in the SO_4–H–SO_4 hydrogen bonds in addition to the O1 atom, as shown in Fig. 1, when these atoms are excluded from calculations. The H1 splitting consistent with our split model from room-temperature results (Sohn *et al.*, 2009) moved the H1 proton from the 9*e* Wyckoff position with a site occupation factor of 1/3 to the 18*h* Wyckoff position with a site occupation factor of 1/6 in TAHS-I. The disorder of the H1 atom has already been postulated by Friese *et al.* (2002), although no displacement from the ideal position could be shown by their X-ray data. Fig. 2 shows the O1—H1—O1 hydrogen-bond network with conventional and split-atom models. The O1—H1 bond lengths of the SO_4–H–SO_4 hydrogen bond are shortened in the split-atom model. They are given in Table 2 for both models and compared with the values obtained for the room-temperature phase TAHS-II.

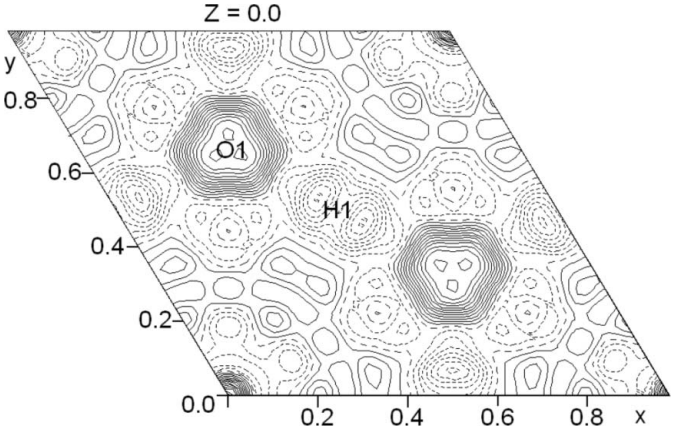

Figure 1
Difference-Fourier map for the O1 and H1 atoms. There is a clear indication of disorder with three split positions for O1 and at least two split positions for H1. Positive contours (solid line) and negative contours (dotted line) are drawn in steps of 0.2 nsl Å^{-3} (nsl = neutron scattering lengths). The negative H density is due to the negative neutron scattering length of the proton.

Table 3
N—H···O hydrogen bond distances (Å) of the split-atom model.

N—H···O	N—H	H···O	N—O	Single/bifurcated
N1—H2···O2	1.04 (1)	1.99 (2)	2.964 (3)	Single
N1—H3···O2	0.82 (4)	2.36 (3)	2.964 (3)	Bifurcated
N2—H4···O2	1.01 (1)	2.10 (1)	3.099 (5)	Single
N2—H5···O2	0.97 (2)	2.13 (1)	3.095 (3)	Single

Two different models were tested to describe the $N1H_4^+$ group properly. First, definite proton positions were searched for around the well localized N1 atom assuming that the $N1H_4^+$ group performs fast librational motions between possible split-atom positions. In doing so a reasonable tetrahedral geometry and acceptable N—H bond lengths were borne in mind. According to the high site symmetry $\bar{3}m$ of the N1 atom, the resulting proton positions reached up to 12 in a split-atom model. The second model was chosen under the assumption that the $N1H_4^+$ group is a freely rotating unit. Rather than 12 split-atom positions with two symmetrically independent H atoms, a continuous proton density on a spherical shell around the N1 position was refined. This model yields a N1—H bond length of 1.08 (4) Å.

While the $N2H_4^+$ tetrahedron is described as completely ordered by Friese *et al.* (2002), we applied a split-atom model for the group owing to the much larger anisotropic displacements. The splitting of H4 into three symmetry-equivalent positions was logical owing to the fact that there were three closest O2 neighbours. Without splitting, each H5 atom forms a bifurcated N—H···O hydrogen bond with two adjacent O2 atoms. This situation changed with splitting and each split H5 atom can be attributed to only one neighbouring O2 atom building single N—H···O hydrogen bonds (Fig. 3). All N—H···O hydrogen bonds between NH_4^+ groups and the nearest SO_4 tetrahedra of the split-atom model are listed in Table 3 with their distances and characters indicating whether the hydrogen bonds are bifurcated or single. The $N1H_4^+$ and $N2H_4^+$ tetrahedra are linked *via* N—H···O hydrogen bonds to the same O2 atoms. Adjacent $N2H_4^+$ tetrahedra of the double

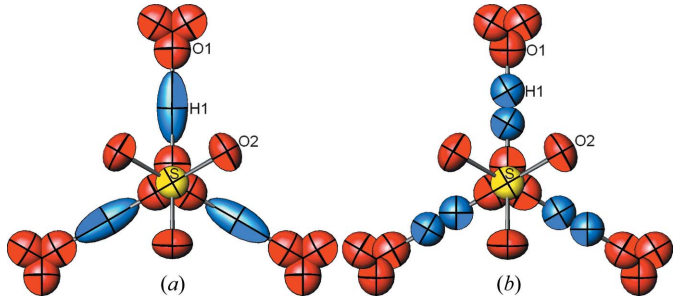

Figure 2
O1—H1—O1 hydrogen bond network in the (001) plane (view along [001]). (*a*) Conventional model; (*b*) split-atom model. Displacement ellipsoids are drawn at the 50% probability level.

layer are also interlinked in the same way by N—H···O hydrogen bonds sharing the same O2 atoms (see Fig. 4).

The disordering of the $N1H_4^+$ and $N2H_4^+$ groups according to the split-atom model are illustrated in Fig. 5. In the split-atom description altogether there are six possible orientations for each NH_4^+ tetrahedron. In Fig. 5, along with the mean NH_4^+ tetrahedra (dashed lines), one specific inclined tetrahedron is drawn for $N1H_4^+$ and $N2H_4^+$ (solid lines). Each H3 atom belongs to one out of six $N1H_4^+$ tetrahedra, whereas the spread out H2 distributions take part in three different $N1H_4^+$ orientations. In the case of $N2H_4^+$ each H4 atom belongs to two orientations and each H5 to three specific $N2H_4^+$ orientations. At this point it is necessary to mention the reason why some H atoms are refined isotropically whereas others are not. Each split atom including O1 and H1 was actually treated both anisotropically and isotropically in several separate refinements and the final results were compared with each other. Sometimes an anisotropic treatment resulted in non-positive definite ADPs (atomic displacement parameters) or showed ADP ellipsoids which have no physical meaning and were too flat. In cases where both treatments were acceptable we carried out the Hamilton test (Hamilton, 1965) and chose the best model in the end. The final weighted R factor of the best split-atom model refined using *JANA*2006 was 0.1091 with 48 refinement parameters. According to the Hamilton test the 'conventional' model can be rejected at the 0.5% level. The spherical shell model refinement performed with *FULLPROF* yielded the final weighted R factor of 0.127 with 41 refinement parameters, whereas the corresponding split-atom model with the same program resulted in a weighted R factor of 0.0764 with 48 parameters. The Hamilton test between these two refinements using *FULLPROF* rejected the spherical shell model at the 0.5% level.

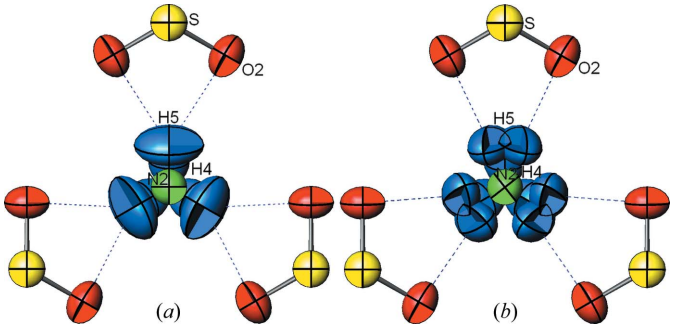

Figure 3
$N2H_4^+$ tetrahedron with the nearest O atoms (view along [001]). (*a*) Bifurcated hydrogen bonds before splitting. (*b*) Single hydrogen bonds with a split-atom model. Displacement ellipsoids are drawn at the 50% probability level.

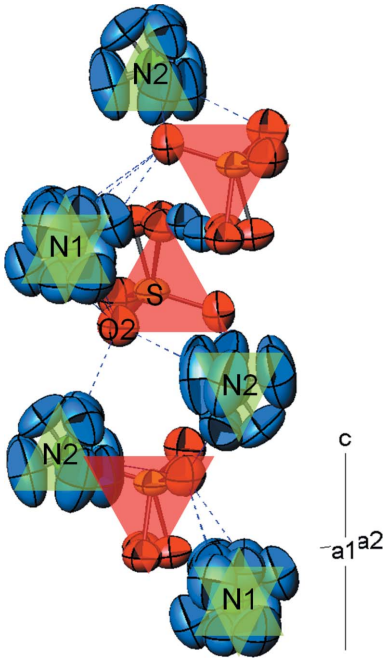

Figure 4
N—H···O hydrogen bonds linking different NH_4^+ groups along the c direction. Displacement ellipsoids are drawn at the 50% probability level.

3.3. Rigid-body analysis of the NH_4^+ groups

Since the protons of the ammonium groups show large ADPs around the well defined N atoms, a rigid-body analysis was performed in order to describe the translational and librational motion of the NH_4^+ groups. An alternative split-atom model was chosen, where all H atoms of both NH_4^+ groups are refined anisotropically. For each $N1H_4^+$ and $N2H_4^+$ group the N1 and N2 atoms were defined as molecule-fixed origins. Owing to the specific site symmetries of N1 ($\bar{3}m$) and N2 ($3m$) there are four independent **T** and **L** parameters for the $N1H_4^+$ group and five independent **T**, **L** and **S** parameters for $N2H_4^+$ (Schomaker & Trueblood, 1968). The **T** and **L** tensors of the NH_4^+ groups are transformed to the crystallographic coordinate system and are listed in Table 4.

Whereas the libration of the $N1H_4^+$ group is isotropic (equal values for the three crystallographic axes), the $N2H_4^+$ group shows much stronger librations around the a/b directions than around c. It is also interesting to note that the libration amplitudes of both $N1H_4^+$ and $N2H_4^+$ groups around the a/b

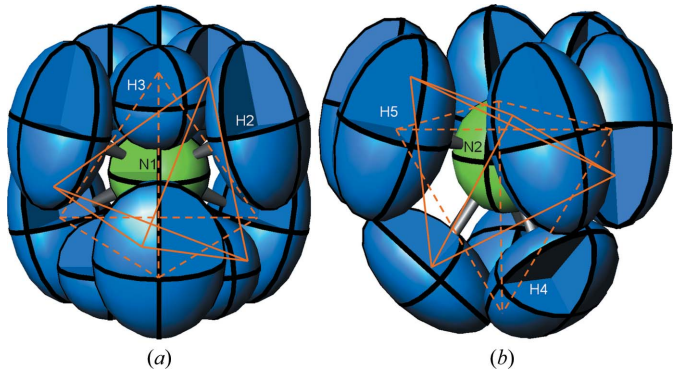

Figure 5
Building principle of one of six possible NH_4^+ tetrahedra. (*a*) $N1H_4^+$ tetrahedron with $\bar{3}m$ symmetry. (*b*) $N2H_4^+$ tetrahedron with $3m$ symmetry. Dashed lines indicate the NH_4^+ tetrahedra orientations for a conventional model and solid lines are examples for NH_4^+ orientations in the split-atom model. Displacement ellipsoids are drawn at the 50% probability level.

Table 4
T (Å^2) and **L** (deg^2) tensors of the NH_4^+ groups of TAHS-I.

	$N1H_4^+$ group	$N2H_4^+$ group
T11	0.069 (1)	0.063 (1)
T22	0.069 (1)	0.063 (1)
T33	0.056 (1)	0.081 (1)
L11	370 (23)	385 (15)
L22	370 (23)	385 (15)
L33	371 (40)	97 (17)

directions are very similar. Fechtelkord *et al.* (2007) previously observed only one nitrogen signal in TAHS-I using ^{15}N MAS NMR spectroscopy and reported that the two N sites experience the same time-averaged chemical environment. The $N2H_4^+$ group loses its high site symmetry 3*m* and takes a general position at the phase transition from TAHS-I to TAHS-II. According to our recent unpublished single-crystal neutron diffraction analyses using the rigid-body treatment, the amplitude of the librational motion of $N2H_4^+$ lowers with decreasing temperature, indicating a freezing of this ammonium group in the low-temperature phases.

3.4. Pathway of superprotonic conductivity

The mechanism of superprotonic conductivity in the $M_3H(XO_4)_2$ structure family has been studied intensively (Baranov *et al.*, 1989; Merinov, 1996; Baranov, 2003). The protonic conductivity of these compounds is distinctly higher in the (001) plane where the main proton transport takes place. As shown in Fig. 6(*b*), a two-dimensional network of hydrogen bonds exists in the high-temperature phase I of TAHS. Contrary to the isolated $(SO_4)H(SO_4)$ dimers in the low-temperature phases, the split O1 atoms in phase I of TAHS are linked by three hydrogen bonds which are equivalent by symmetry. Every H1 atom has a site occupation factor of 1/6 (1/3 for each double-minimum hydrogen bond) and allows proton diffusion in the (001) plane. This proton diffusion process occurs in two steps:

(i) proton transfer takes place between the two potential minima of the SO_4-H-SO_4 hydrogen bonds;

(ii) an existing hydrogen bond is broken and the proton moves to a neighbouring available site, forming a new hydrogen bond.

In earlier literature the formation energy of a hydrogen bond and the energy of a proton transfer between two potential minima of a hydrogen bond were studied as functions of the O···O distance in the approximation of an isolated linear hydrogen bond (Yomosa & Hasegawa, 1970; Lippincott & Shroeder, 1955). As a result the optimum condition for a fast proton diffusion is obtained if the O···O distance lies between 2.6 and 2.7 Å, and this is exactly the case for TAHS-I where the O1···O1 distance is 2.675 (8) Å.

A possible involvement of the NH_4^+ groups in proton conduction in TAHS-I was proposed by Merinov *et al.* (2000). They calculated the low potential barrier energy for an exchange of protons between the hydrogen bonds and the NH_4^+ groups. This model assumption was supported by Fechtelkord *et al.* (2000) with two-dimensional ^{1}H NOESY MAS NMR experiments. In their work they found clear evidence of chemical exchange between acidic protons of the hydrogen bonds and ammonium protons. Since the $N1H_4^+$ group is located in the pseudo-hexagonal network of hydrogen bonds in the (001) plane it is most likely that the protons of this ammonium group are involved in the superprotonic conduction of TAHS-I. From our single-crystal neutron diffraction analysis we show nuclear density maps to illustrate the variation of H2 proton distribution related to the H1 atoms of the hydrogen bonds in the (001) plane (Fig. 6). The nuclear density maps at $z = \pm 0.01$ show a clear correlation between displacements of the H1 atoms in the hydrogen bonds and displacements of the H2 atoms of the $N1H_4^+$ groups. The elongation of the displacement ellipsoids for the H1 atoms of the hydrogen bonds, and for the H2 atoms from the $N1H_4^+$

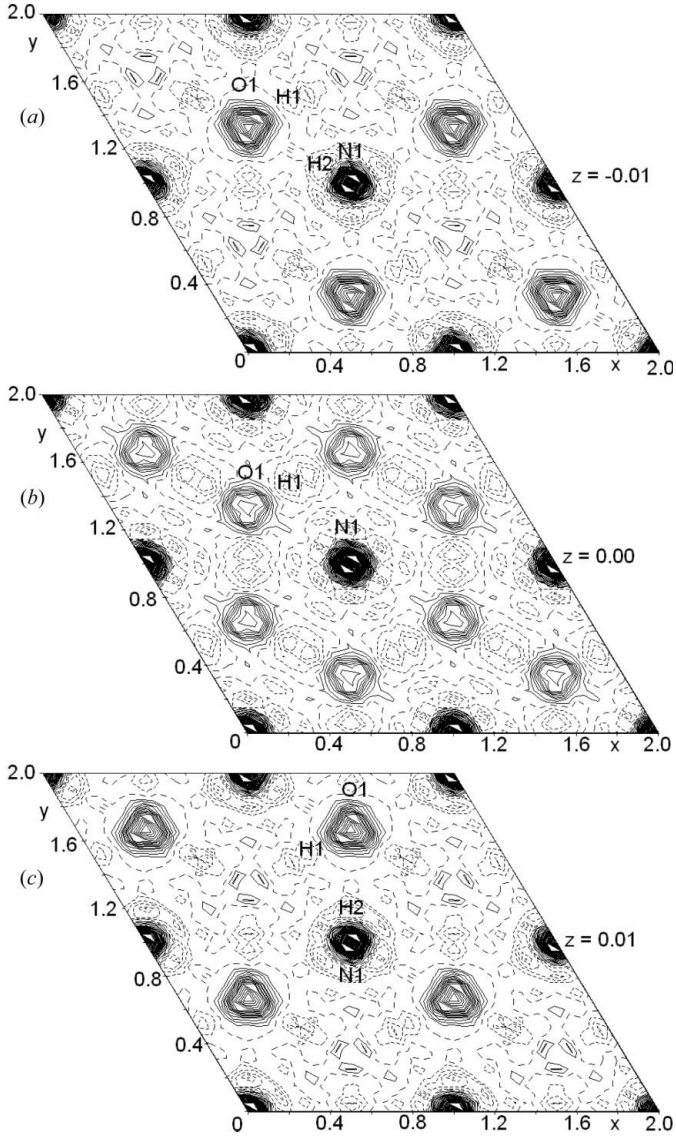

Figure 6
Nuclear density map F_{obs} of hydrogen bonds in the (001) plane. (*a*) $z = -0.01$; (*b*) $z = 0.00$; (*c*) $z = 0.01$. Positive contours (solid line) and negative contours (dotted line) are drawn in steps of 0.5 nsl Å^{-3}.

groups perpendicular to the O1—H1 and N1—H2 bond directions support proton diffusion between the SO_4—H—SO_4 hydrogen bonds and the $N1H_4^+$ groups. The distance between H1 protons of adjacent hydrogen bonds is 2.31 (2) Å (see Fig. 6*b*) and the distance between H1 and H2 protons is 2.25 (1) Å (Figs. 6*a* and *c*).

4. Conclusions

Using single-crystal neutron diffraction a more detailed crystal structure analysis of the high-temperature phase I of TAHS with special emphasis on the proton distribution is performed. The disorder of the O1 atom taking three symmetrically equivalent split positions is characteristic for TAHS-I, allowing a pseudo-hexagonal network of hydrogen bonds in the (001) plane. With an O1···O1 distance of 2.675 (8) Å typical for a strong hydrogen bond the proton migration condition between two potential minima is given. Additional O1 dynamic disorder allows for the diffusion of the protons between adjacent hydrogen bonds. Moreover, the short distance between H1 positions of SO_4—H—SO_4 hydrogen bonds and H2 from the $N1H_4^+$ group is also in favour of a supplementary proton exchange with the ammonium protons. H1 splitting directly resulted from difference-Fourier maps and gave rise to a split-atom position on the 18*h* Wyckoff position with a site occupation factor of 1/6. Regarding the strongly enlarged anisotropic mean-square displacements of the protons of the NH_4^+ groups, further splitting of the H protons was carefully tested and the best result according to the Hamilton test, as well as considering an acceptable physical meaning, is presented in this paper. Throughout the unit cell the NH_4^+ groups build N—H···O hydrogen bonds with adjacent SO_4 tetrahedra and they are linked among each other by sharing the same O2 atoms of these hydrogen bonds. A rigid-body analysis using TLS tensors provided a motional picture of the translational and librational behaviour of the NH_4^+ groups.

References

Baranov, A. I. (2003). *Crystallogr. Rep.* **48**, 1012–1037.

Baranov, A. I., Merinov, B. V., Tregubchenko, A. V., Khiznichenko, V. P., Shuvalov, L. A. & Schagina, N. M. (1989). *Solid State Ionics*, **36**, 279–282.

Chen, R. H., Chen, T. M. & Shern, C. S. (2000). *J. Phys. Chem. Solids*, **61**, 1399–1406.

Dominiak, P. M., Herold, J., Kolodziejski, W. & Woźniak, K. (2003). *Inorg. Chem.* **42**, 1590–1598.

Dowty, E. (2000). *ATOMS* for Windows, Version 5.1. Shape Software, Kingsport, Tennessee, USA.

Fechtelkord, M., Diekmann, A. & Bismayer, U. (2007). *Am. Mineral.* **92**, 1821–1826.

Fechtelkord, M., Engelhardt, A., Buhl, J. C., Schwalowsky, L. & Bismayer, U. (2000). *Solid State Nucl. Magn. Reson.* **17**, 76–88.

Fischer, P. (1914). *Z. Kristallogr.* **54**, 528–531.

Friese, K., Aroyo, M. I., Schwalowsky, L., Adiwidjyjy, G. & Bismayer, U. (2002). *J. Solid State Chem.* **165**, 136–147.

Gesi, K. (1976). *Phys. Status Solidi*, **33**, 479–482.

Gesi, K. (1980). *Jpn. J. Appl. Phys.* **19**, 1051–1053.

Gossner, B. (1904). *Z. Kristallogr.* **38**, 110–168.

Hamilton, W. C. (1965). *Acta Cryst.* **18**, 502–510.

Hahn, Th. (2002). *International Tables for Crystallography*, Vol. A. Dordrecht: Kluwer Academic Publishers.

Heger, G., Mullen, D. & Knorr, K. (1975). *Phys. Status Solidi A*, **31**, 455–462.

Lippincott, E. & Shroeder, R. (1955). *J. Chem. Phys.* **23**, 1099–1106.

Merinov, B. V. (1996). *Solid State Ionics*, **84**, 89–96.

Merinov, B., Bourenkov, G. & Bismayer, U. (2000). *Phys. Status Solidi*, **218**, 365–378.

Petricek, V., Dusek, M. & Palatinus, L. (2006). *JANA*2006. Institute of Physics, Praha, Czech Republic.

Rodriguez-Carvajal, J. (2001). *CPD Newsl.* **26**, 12–19.

Scherf, C. (1998). *PRON*, Revised Stoe Version. Institute of Crystallography, Aachen, Germany.

Schomaker, V. & Trueblood, K. N. (1968). *Acta Cryst.* B**24**, 63–76.

Schwalowsky, L., Vinnichenko, V., Baranov, A., Bismayer, U., Merinov, B. & Eckold, G. (1998). *J. Phys. Condens. Matter*, **10**, 3019–3027.

Sohn, Y. J., Loose, A., Merz, M., Sparta, K., Klapper, H. & Heger, G. (2009). *Acta Cryst.* B**65**, 36–44.

Yomosa, S. & Hasegawa, M. (1970). *J. Phys. Soc. Jpn*, **29**, 1329–1334.